Equatorial ionosphere semiannual oscillation investigated from Schumann resonance measurements on board the C/NOFS satellite

Fernando Simões,[1] Robert Pfaff,[1] Henry Freudenreich,[1,2] Jeffrey Klenzing,[1] Douglas Rowland,[1] Kenneth Bromund,[1] Larry Kepko,[1] Guan Le,[1] Maria Carmen Liebrecht,[3] Steven Martin,[1,2] and Paulo Uribe [1]

Received 2 October 2012; revised 19 August 2013; accepted 25 August 2013; published 12 November 2013.

[1] Detection of Schumann resonance signatures in the equatorial ionosphere offers remote sensing capabilities for the investigation of tropospheric and space weather effects in the ionosphere. Schumann resonances are electromagnetic oscillations in the earth-ionosphere cavity produced by lightning activity. Analysis of AC electric field measurements gathered by the Communications/Navigation Outage Forecasting System satellite reveals a semiannual pattern in Schumann resonance data recorded during nighttime in the equatorial ionosphere. This pattern observed in the Schumann resonance amplitude is expected to help validate—or at least constrain—potential mechanisms proposed to explain the semiannual oscillation observed in different geophysical records, such as those reported in a variety of tropospheric, ionospheric/thermospheric, and magnetospheric observations.

Citation: Simões, F., et al. (2013), Equatorial ionosphere semiannual oscillation investigated from Schumann resonance measurements on board the C/NOFS satellite, *J. Geophys. Res. Atmos.*, *118*, 12,045–12,051, doi:10.1002/jgrd.50797.

1. Introduction

[2] The dynamics of the ionosphere is driven by the solar wind, geomagnetic activity, and in situ aeronomy processes, as well as by forcing from below. Continuous and transient phenomena influence the density of the ionosphere/thermosphere at local and global scale, namely plasma mixing, heating, and ionization induced by solar Extreme Ultraviolet (EUV) radiation, cosmic rays, magnetospheric sources, gravity waves, tides, and lightning. Among a variety of short- and long-term patterns observed in the ionosphere, the semiannual variability of neutrals and plasma density has been known for decades but remains poorly understood. Semiannual patterns have been found in not only ionospheric but also tropospheric and magnetospheric data. On average, the density of the thermosphere is lower during solstice; comparable variation is observed in the O/N_2 ratio. A rather similar feature is identified in the ionospheric plasma density.

[3] Seasonal variability of the F_2 layer electron density peak, N_mF_2, has been studied since the dawn of ionospheric research [*Appleton and Naismith*, 1932]. A semiannual periodicity is observed in not only plasma parameters but also neutrals composition [*Paetzold and Zschorner*, 1961]. The mechanism generally accepted for the F_2 layer seasonal patterns involves changes in neutrals composition [*Rishbeth and Setty*, 1961; *Fuller-Rowell*, 1998; *Rishbeth et al.*, 2000]. A quantitative explanation of the phenomenon must involve both ionospheric and thermospheric processes, for example, total EUV solar flux is responsible for ionization and heating and induces neutral composition changes as well. Although some features are successfully represented in ionospheric and thermospheric empirical models such as the International Reference Ionosphere (IRI) [*Bilitza and Reinisch*, 2009] and the Mass Spectrometer and Incoherent Scatter (MSIS) [*Picone et al.*, 2002], a comprehensive description of the mechanism is still lacking. A semiannual oscillation peaking at the equinoxes is also observed in lightning [e.g., *Kandalgaonkar et al.*, 2005], thunderstorm [e.g., *Williams*, 1994], and geomagnetic activity [e.g., *Chapman and Bartels*, 1940]. Moreover, Schumann resonance spectral signatures measured on the ground follow similar patterns [*Sátori and Zieger*, 1996]. Evidence of a link between the intensity of Schumann resonance and global surface temperature variability has been reported; measurements show a strong annual variation in the Schumann resonance intensity, while the semiannual component prevails in the tropics and subtropics [*Sekiguchi et al.*, 2006]. Additionally, *Füllekrug and Fraser-Smith* [1997] report characteristics of global lightning activity on a seasonal time scale from ELF magnetic field measurements. The resulting mean seasonal variations of continental lightning in mid and tropical latitudes are found to be related to surface temperature variations. Stratospheric and mesospheric zonal winds show semiannual periodicity, peaking near the stratopause [e.g., *Reed*, 1966]. Gravity wave kinetic energy, as well as variances in each of the three component wind directions, shows a semiannual

[1]Heliophysics Science Division Space Weather Laboratory, NASA/GSFC, Greenbelt, Maryland, USA.
[2]ADNET Systems, Inc, Rockville, Maryland, USA.
[3]Sigma Space Corporation, Lanham, Maryland, USA.

Corresponding author: F. Simoes, Heliophysics Science Division, Space Weather Laboratory (code 674), NASA/GSFC, 8800 Greenbelt Road, Greenbelt, MD 20771, USA. (fernando.a.simoes.nasa@gmail.com)

2169-897X/13/10.1002/jgrd.50797

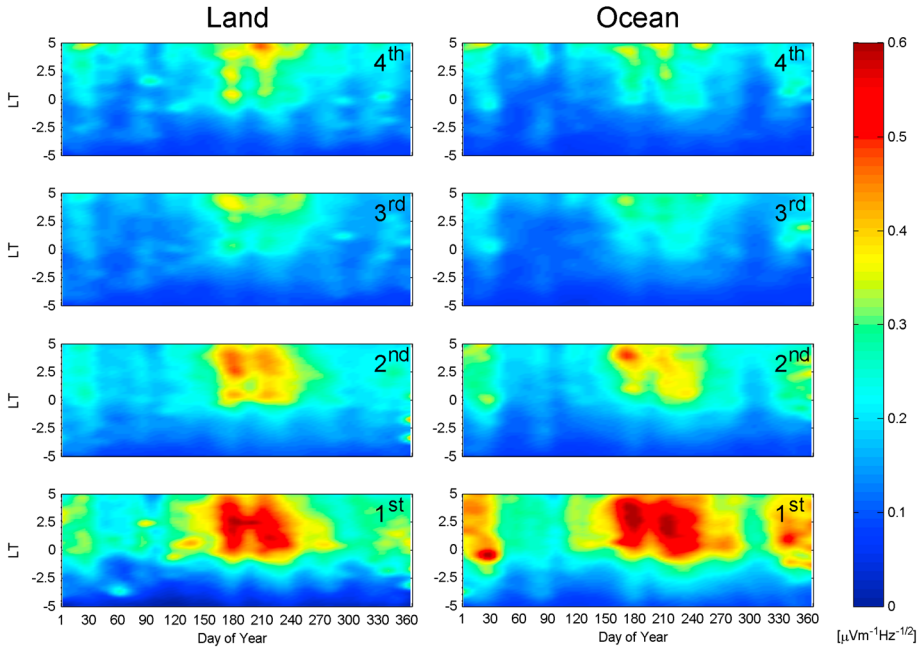

Figure 1. Average amplitudes of the lowest four eigenmodes of Schumann resonance as a function of LT and DOY for longitudes corresponding to (left column) land and (right column) ocean as explained in the text. LT is centered on midnight. The data set corresponds to about 16,500 C/NOFS orbits (May 2008–May 2011), which correspond to conditions of low solar activity.

variation in the mesosphere with maxima and minima during solstice and equinox, respectively [e.g., *Meek et al*., 1985]. A complete description of the mechanisms responsible for the semiannual variability observed in multiple layers of the Earth gaseous envelope, from the troposphere to the magnetosphere, is still unavailable. Whether these semiannual patterns are different manifestations of the same mechanism or a mere coincidence is even more difficult to ascertain.

[4] The period of low solar activity between solar cycles 23 and 24 offers unique conditions for investigating space weather in the near-Earth environment, mainly aerodynamic and electrodynamic processes in a highly contracted atmosphere. During 2008 and 2009, solar activity reached the lowest levels observed during the space age, offering unprecedented stable conditions to study ionospheric and thermospheric phenomena. In this work, we present Extremely Low Frequency (ELF) electric field data recorded by the Vector Electric Field Investigation (VEFI) on board the Communications/Navigation Outage Forecasting System (C/NOFS) satellite [*de la Beaujardière et al*., 2004]. Analysis of these electric field measurements shows a semiannual periodicity in the amplitude of Schumann resonances, unveiling new techniques to investigate ionospheric/thermospheric dynamics.

2. Schumann Resonance Measurements

[5] Schumann resonances are electromagnetic oscillations in the earth-ionosphere cavity and are generated by lightning activity. The normal mode frequencies (eigenfrequencies) of order n, ω_n, of a lossless, thin spherical cavity can be, to a first approximation, computed from $\omega_n = \sqrt{n(n+1)c/R}$, where c is the velocity of light in vacuum, R is the average radius of the cavity, and $n = 1, 2, 3,\ldots$ the corresponding order of the mode of the cavity [e.g., *Nickolaenko and Hayakawa*, 2002]. Investigations of Schumann resonance have been used to assist with the characterization of a variety of phenomena related to atmospheric electricity, namely electromagnetic wave propagation in the atmosphere and lightning climatological studies. Detection of Schumann resonance signatures in the equatorial ionosphere on board the C/NOFS satellite provides remote sensing capabilities to investigate atmospheric electricity and ELF wave propagation from orbit [*Simões et al*., 2011, 2012a].

[6] C/NOFS was launched in April 2008 and inserted into an elliptical orbit of 401 km perigee, 852 km apogee, and 13° inclination, and includes instrumentation for measuring the electron and ion densities and temperatures, DC electric and magnetic fields, the ion velocity and lightning flash rates, and low-frequency electric field waves. The period of the C/NOFS orbit is about 95 min and the apogee has been slowly decreasing over time. The satellite is equipped with a vector double probe experiment with three, orthogonal pairs of 20 m tip-to-tip booms [*Pfaff et al*., 2010]. The broadband ELF electric field waveforms are recorded at 512 samples/s with 16 bit analog to digital converters and are then telemetered to the ground where they may subsequently undergo spectral processing and rotation into different coordinate systems. Sometimes only one of those components is available due to telemetry constraints. In this study, we use component E34, which is gathered more often and hence provides a robust data set. (The E34 component corresponds to the electric field component between spheres 3 and 4 and is located in the orbital plane and is roughly perpendicular to the ambient magnetic field.) Since Schumann resonance detection is most conspicuous in the nighttime data, in this study, we exclude the period 5–19 Local Time (LT) from our analysis.

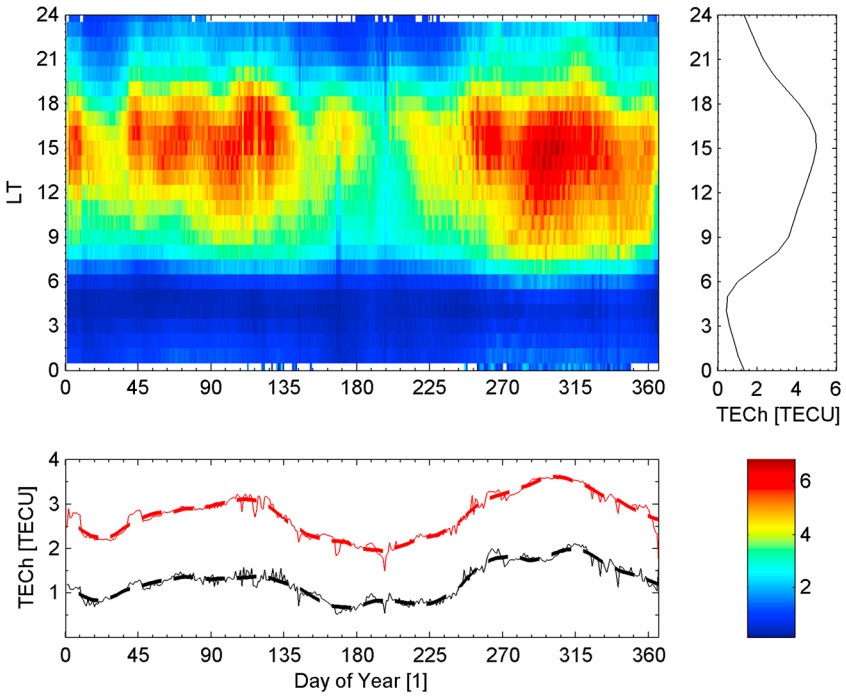

Figure 2. Total electron content, represented by TECh and computed with the IRI empirical model from May 2008 to May 2011 at the position of C/NOFS, whenever ELF data are available, is shown as a function of LT and DOY in the top panel on the left. See text for the definition of TECh. The top panel (right) represents the TECh averaged over DOY. The red and black curves in the bottom panel represent mean TECh computed over 0–24 LT and 19–5 LT, respectively, as a function of DOY. Some vertical narrow features seen in the bottom panel as well as in the map, e.g., near days 40–50 and 200, correspond to uneven distribution of the ELF data set. The dashed lines are obtained after applying a Savitzky-Golay smoothing filter.

[7] Figure 1 shows the lowest four modes of the Schumann resonance amplitude over land and sea, averaged from May 2008 to May 2011, as a function of LT and Day of Year (DOY). Given the low inclination of C/NOFS, all longitudes and local times are evenly covered throughout the mission. To a first approximation, the longitude sectors (0°–55°, 95°–165°, 280°–330°, 355°–360°) and (55°–95°, 165°–280°, 330°–355°) correspond to land and ocean, respectively. The main features revealed by the average Schumann resonance spectral signatures shown in this Figure include (i) presence of a semiannual pattern, (ii) largest amplitudes during northern summer solstice, (iii) significantly larger amplitude in the postmidnight sector, (iv) amplitude generally decreasing with the cavity mode—slight increase in the amplitudes in mode 4 compared to mode 3 is an exception, and (v) similar amplitude variability through DOY for all modes; and (vi) similar amplitude over the land and ocean sectors.

3. Discussion

[8] Detection of Schumann resonance signatures in the ionosphere offers remote sensing capabilities to investigate not only lightning climatology but also ionosphere variability. Combining ground-based and satellite measurements, we can study ELF electromagnetic oscillations in the earth-ionosphere cavity as well as wave attenuation in the ionosphere. Since the wavelength associated with Schumann resonance phenomena is commensurate with the size of the cavity, these ELF spectral features can be used to assess atmospheric and ionospheric properties at a regional and global scale. Thus, analysis of VEFI data may help validate—or at least constrain—the various mechanisms proposed to explain the semiannual periodicity observed in several types of geophysical records.

[9] To contrast ionospheric and thermospheric parameterizations with Schumann resonance measurements made by VEFI in the equatorial ionosphere, we evaluate relevant parameters of the IRI and MSIS empirical models at the location of the satellite throughout the mission, with a 10 min resolution. Since the electromagnetic source is located in the troposphere and the amplitude of Schumann resonance is directly linked to properties of the ionosphere as well as distance to the source, we use TECh instead of the Total Electron Content (TEC) to provide a more suitable comparison with VEFI measurements. TECh defines the electron content present in a vertical column integrated from the ground up to the altitude of the satellite, i.e., a major fraction of TEC. It is important to mention that the ELF data set is not strictly continuous in the time span considered, but data gaps do not weaken the quality of the analysis.

[10] To compare Schumann resonance amplitude with ionospheric and thermospheric characteristics, we compute the average TECh from IRI at the satellite location as a function of DOY and LT, as shown in Figure 2 for the period from May 2008 to May 2011. Averages of TECh for two LT periods (0–24 and 19–5 h) as a function of DOY are also provided to emphasize key features, namely the semiannual variability and the day-night dichotomy.

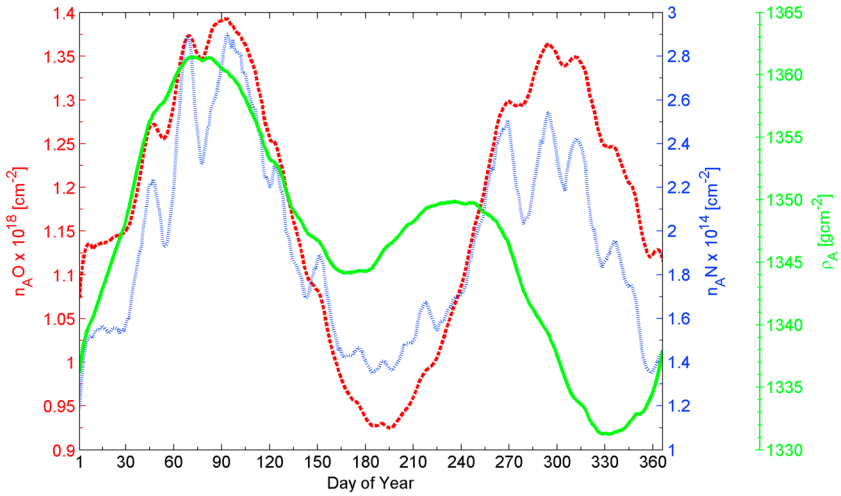

Figure 3. Average area number density of atomic oxygen (n_AO, red/dashed curve) and nitrogen (n_AN, blue/dotted curve) as well as area density of neutrals (ρ_A, green/solid curve) computed with the MSIS empirical model. Number density is integrated over a column extending from the ground up to the altitude of the satellite, whenever ELF data are available. In addition to the prominent semiannual pattern, smaller features (e.g., ~25 day periodicity) seen in n_AO and n_AN are caused by the C/NOFS perigee precession through latitude as well as due to a minor uneven distribution of the ELF data set during the time span considered.

[11] The average area number density of atomic oxygen (n_AO) and nitrogen (n_AN), as well as area mass density of neutrals (ρ_A), integrated from the ground up to the altitude of the satellite using the MSIS empirical model, is shown in Figure 3, in a presentation similar to the lower panels of Figure 2. This integration aims to identify a possible cumulative effect of neutral density in electromagnetic wave attenuation possibly related to its connection to collision frequency since, for example, the Pedersen and Hall conductances are a function of charged-neutral collision frequency.

[12] Semiannual patterns have been identified in magnetospheric, ionospheric, and tropospheric data, corresponding to modification of medium properties from a few percent to threefold. Semiannual variability of average density of neutrals integrated from the troposphere up to the thermosphere is typically 2–3% (Figure 3). A similar periodicity is observed in geomagnetic activity with ~20% peak-to-peak amplitude variation in the *Dst* magnetic index [e.g., *Russell and McPherron*, 1973]. However, semiannual oscillations are stronger in thermospheric and ionospheric data. For example, difference in atomic oxygen number density is about 50% and TEC can reach a twofold variation. Annual and semiannual patterns are also prominent in ground-based ELF measurements, where the solstice to solstice and solstice to equinox ratios of the Schumann resonance amplitude can reach ~2.5 and ~1.5, respectively [*Märcz et al.*, 1997].

[13] Semiannual patterns from the troposphere up to the magnetosphere have been recognized for a long time, but the mechanism (or mechanisms) responsible for these patterns remains elusive. Depending on the geophysical data set, several interpretations have been proposed and explored to explain the periodicity. Some explanations involve celestial mechanics, tilt of the magnetic dipole axis, and variations in H^+ scale height in the plasmasphere induced by magnetospheric phenomena [e.g., *Russell and McPherron*, 1973]. Several models consider plasma and aeronomy processes including variability of O^+ levels in the upper ionosphere, chemical equilibrium levels of H^+ in the topside ionosphere, changes in production and loss rates in the upper ionosphere where transport processes dominate, variation of ionospheric neutrals composition, and asymmetric geographic distribution in the ionosphere of production rate and loss of atomic oxygen [e.g., *Rishbeth and Setty*, 1961; *Fuller-Rowell*, 1998; *Richards*, 2001; *Mikhailov and Perrone*, 2011]. Other models invoke aerodynamic processes in the atmosphere, namely variation in mean tropospheric winds enabling a gravity wave modulation of tidal amplitudes, and modifications in thermospheric neutral wind patterns due to local heating [e.g., *Hirota*, 1980; *Garcia et al.*, 1997; *Mayr et al.*, 1998]. Variations in oceanic and tropospheric hydrological/thermodynamic parameters have been also proposed to explain specific semiannual variations in the Earth gaseous envelope, namely Schumann resonance and lightning-related patterns [e.g., *Williams*, 1994; *Nickolaenko and Rabinowicz*, 1995; *Sátori and Zieger*, 1996; *Sekiguchi et al.*, 2006]. Orbital mechanics, for example, may give an indication why N_mF_2 is lower in June than in December, but a ~3% variation in the Sun-Earth distance, and consequently ~7% in solar flux, is insufficient to explain a ~50% change in electron density. Furthermore, orbital eccentricity is consistent with an annual periodicity of N_mF_2 but cannot accurately explain the semiannual pattern. Multidisciplinary approaches are therefore necessary to provide a complete analysis of the impact of the semiannual periodicity in the Earth environment, both from tropospheric and space weather perspectives.

[14] A priori, the semiannual periodicity of the Schumann resonance amplitude revealed by VEFI could be attributed to seasonality of lightning, distance from the satellite to the source, variability of ionospheric plasma, or characteristics of wave propagation. To understand the nature of the Schumann resonance semiannual variability identified in C/NOFS data, we compare VEFI measurements with IRI and MSIS estimates as a function of LT and DOY. Qualitatively, the main TEC

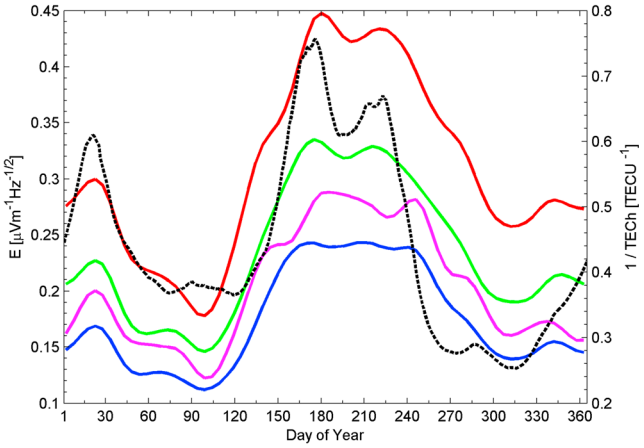

Figure 4. Average amplitude of the electric field, *E*, of the lowest Schumann resonance modes (first: red, second: green, third: blue, and fourth: magenta) as a function of DOY, derived from Figure 1. The black dotted curve represents the reciprocal of average TECh computed from Figure 2 for the range 19–5 LT.

morphological features of the ionosphere as a function of DOY are similar to those derived from integrating the electron content up to 400, 850 km, or altitude of the satellite. Since the electromagnetic source is located in the troposphere and Schumann resonance features observed in the ionosphere are linked to ionospheric plasma properties, we consider TECh instead of TEC to provide a more suitable comparison with VEFI measurements.

[15] Figure 4 shows the amplitude of Schumann resonance and the reciprocal of TECh as a function of DOY. The maximum-to-minimum ratio of the Schumann resonance amplitude semiannual pattern is in the range 2.1–2.5 for all the modes considered. Note a strong correlation between 1/TECh and the Schumann resonance modes. Comparison between the same variables as a function of LT is presented in Figure 5. The Schumann resonance amplitude in the postmidnight sector is larger for the four modes, but there is a ~2 h offset between modes 1–2 and 1/TECh calculated from IRI. Several scenarios may contribute to explain such offset. First, according to C/NOFS measurements, plasma irregularities have been identified more frequently in the postmidnight sector during 2008 and 2009 [e.g., *Pfaff et al.*, 2010]. For example, using a radio beacon on board C/NOFS, *Thampi et al.* [2009] show significant spread-F taking place in the altitude range 200–400 km at 1–3 LT. Second, similar differences between IRI predictions and measurements are also sometimes noticed in GPS measurements in the equatorial ionosphere [e.g., *Adewale et al.*, 2012]. Third, the oxygen gyrofrequency falls in the ELF range and perhaps modifies wave propagation conditions in the ionosphere. Fourth, performance of IRI is worst at dawn during extreme solar minimum conditions [*Klenzing et al.*, 2011]. According to the amplitude of Schumann resonance modes presented in Figure 5 and other ELF phenomena (e.g., ionospheric Alfvén resonator and hiss signatures) observed by VEFI [*Simões et al.*, 2012b], spectral morphological transitions occur at about 20 Hz, perhaps related to the O^+ gyrofrequency. From SR ground measurements in California and Western Australia, *Sentman and Fraser* [1991] observed a *D* region minimum height occurring at approximately 1300–1400 LT. Although those measurements refer to daytime conditions and the illumination conditions are reversed, we can recognize a 1–2 h lag in the density peak, similar to that observed by C/NOFS during nighttime conditions. A comparison of C/NOFS and ground-based measurements with electron density derived from IRI suggests plasma drifts and neutrals transport due to the Earth rotation contribute to explain the offset. However, more elaborate analyses are necessary to identify and fully characterize potential mechanisms.

[16] A comparison between Figures 3 and 4 shows significant correlation or anticorrelation among several physical parameters. Specifically, the Pearson product-moment correlation coefficient between the Schumann resonance amplitude and 1/TECh, n_AO, and ρ_A is approximately 0.67, −0.86, and −0.17, respectively; for reference, the critical value of the Pearson product-moment correlation coefficient for this sample is 0.3 with a level of significance of 10^{-6} (about 5σ), and correlation between Schumann resonance modes is ~0.98. Although correlation with 1/TECh would be expected since wave attenuation increases with the electron content and electrical conductivity, a strong correlation (anticorrelation, in this case) between the Schumann resonance amplitude and number density of atomic oxygen is somewhat surprising. This result suggests that aeronomy effects may play a fundamental role in the mechanism responsible for the Schumann resonance semiannual pattern observed in the equatorial ionosphere during nighttime. *Mikhailov and Perrone* [2011] suggest that seasonal differences in daytime N_mF_2 solar activity variations are due to specific roles that the neutral composition (O, O_2, and N_2) and temperature play during solstices, and therefore the observed seasonal difference in N_mF_2 cannot simply be reduced to seasonal O/N_2 changes. Additionally, they also claim that the December anomaly in N_mF_2, for example, is not purely a daytime effect; global N_mF_2 increase also takes place during the night when direct photoionization is absent, suggesting that the present results may be pertinent, at least qualitatively, to daytime conditions as well. Although increasing considerably with solar activity, it has been reported that the absence of significant seasonal differences in midlatitude daytime N_mF_2 close to solar minimum [e.g., *Sethi et al.*, 2002]; according to Schumann resonance, VEFI measurements are

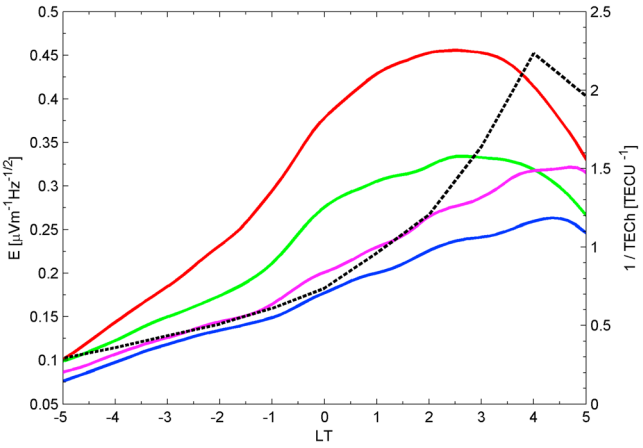

Figure 5. Same caption as in Figure 4 as a function of LT.

not the case for the nighttime equatorial region between solar cycles 23 and 24 under extreme solar minimum conditions.

[17] Contrasting VEFI measurements with ground-based Schumann resonance records contribute to assessing robustness of the present data set. First, it is important to emphasize that the Schumann resonance amplitude variation observed in the ionosphere as a function of DOY is not affected by lightning geographic distribution because the equatorial region is evenly sampled. *Sátori and Zieger* [1996] recorded the ELF electric field vertical component during 1993–1995 at the Nagycenk Observatory, Hungary, and observed a semiannual variability of Schumann resonance amplitude. The three modes reported show an amplitude decrease with mode increase corroborating our results; the third mode is not in phase with the lower modes but, according to the authors of that study, its significance may be limited. Subsequent work by *Märcz et al*. [1997] at the same observatory shows Schumann resonance seasonal variability in a better agreement with measurements in the ionosphere. Although comparisons with ground-based measurements must be made cautiously because the geographic coverage is different, an important result is observation of similar solstice to solstice and solstice to equinox ratios of the Schumann resonance amplitude on the ground and in the ionosphere. Comparison of the VEFI data set with more recent, robust ground-based measurements would be invaluable for investigating the cavity leakage mechanism and ELF wave propagation in the ionosphere, as well as constraining mechanisms proposed to explain the semiannual patterns observed in tropospheric, ionospheric, and magnetospheric data. The observed plasma density alone is not sufficient for explaining the cavity leakage, but the anisotropy of the cavity must be considered as well [*Madden and Thompson*, 1965]. Although medium parameterization requires significant improvements, they predict a clear day-night dichotomy regarding ELF wave propagation conditions in the ionosphere.

[18] After assessing several tropospheric and ionospheric phenomena showing semiannual periodicities, it is possible to estimate their significance for the Schumann resonance pattern observed on board C/NOFS. The amplitude of the Schumann resonance modes in the ionosphere peaks during the solstices, but *Christian et al*. [2003] found some evidence that the semiannual cycle peaks near the equinoxes, with the autumnal equinox dominating. Nevertheless, as shown in Figure 4, the SR peaks are wider than that derived from the reciprocal of average TECh. This result may also suggest a contribution from global lightning activity, which reaches a maximum in August. Lightning is more prevalent in the late afternoon and over land [e.g., *Christian et al*., 2003], but amplitude of the Schumann resonance modes is larger after midnight and quite similar in the land and ocean sectors. Conversely, a similar response observed in the Schumann resonance amplitude and 1/TECh suggests that ELF wave attenuation in the ionosphere is more pertinent than lightning intensity and distribution inside the cavity. The most interesting result is perhaps the significant anticorrelation between the number density of atomic oxygen and the Schumann resonance periodicity, as well as the contrast between modes 1–2 and 3–4 in the postmidnight sector. Since neutral number density (via collision frequency) and ion composition are relevant to estimate the Pedersen and Hall conductivities [*Madden and Thompson*, 1965], these results may be useful to investigate the leakage mechanism by providing a better assessment of the medium anisotropy. In addition to accurate modeling of wave propagation conditions in the ionosphere, it is important to understand the extent of the contribution by lightning toward the observed SR semiannual periodicity. Future studies will investigate how the spatial and temporal distribution of lightning influences the resultant SRs in a given ionospheric cavity.

4. Conclusion

[19] Detection of Schumann resonance signatures in the equatorial ionosphere offers remote sensing capabilities to investigate atmospheric electricity as well as ELF wave propagation in the ionosphere. Analysis of AC electric field measurements gathered by the VEFI instrument on the C/NOFS satellite reveals a semiannual pattern in Schumann resonance data. The main Schumann resonance spectral features are (i) presence of a semiannual periodicity, (ii) larger amplitude during northern summer solstice, (iii) significantly larger amplitude in the postmidnight sector, (iv) amplitude decreasing with the cavity modes—misplacement between modes three and four is an exception, (v) similar amplitude variability through DOY for the lowest four modes, and (vi) similar amplitudes over the land and ocean longitude sectors. Additionally, correlation of Schumann resonance semiannual patterns with the reciprocal of TECh and number density of atomic oxygen seems particularly relevant. These results suggest that the Schumann resonance amplitude semiannual variability is mainly driven by plasma properties and wave propagation in the ionosphere rather than by lightning distribution. Modeling cavity leakage of ELF waves is important for providing quantitative assessments of the SR semiannual pattern, and possibly to identify and characterize the mechanisms that generate such periodicity. Although significant improvements are necessary to bring models and C/NOFS data to an agreement, the studies by *Grimalsky et al*. [2005] and, notably, *Madden and Thompson* [1965] offer a reasonable starting point for modeling ELF wave propagation in the ionosphere. A complete description of the mechanism responsible for the semiannual oscillation detected in multiple geophysical records—from the troposphere up to the magnetosphere—remains elusive. The pattern observed in the Schumann resonance amplitude is expected to help validate—or at least constrain—potential mechanisms previously proposed to explain the semiannual oscillation.

[20] **Acknowledgments.** The Communication/Navigation Outage Forecast System (C/NOFS) mission, conceived and developed by the U.S. Air Force Research Laboratory, is sponsored and executed by the USAF Space Test Program. We acknowledge support from the Air Force Office of Scientific Research. FS is supported by an appointment to the NASA Postdoctoral Program at the Goddard Space Flight Center, administered by Oak Ridge Associated Universities through a contract with NASA.

References

Adewale, A. O., E. O. Oyeyemi, P. J. Cilliers, L. A. McKinnell, and A. B. Adeloye (2012), Low solar activity variability and IRI 2007 predictability of equatorial Africa GPS TEC, *Adv. Space Res.*, *49*, 316–326.

Appleton, E. V., and R. Naismith (1932), Some measurements of upper-atmospheric ionisation, *Proc. R. Soc. London Ser. A*, *137*, 36–54, doi:10.1098/rspa.1932.0119.

Bilitza, D., and B. W. Reinisch (2009), International Reference Ionosphere 2007: Improvements and new parameters, *Adv. Space Res.*, *44*, 701–706.

Chapman, S., and J. Bartels (1940), *Geomagnetism*, Oxford University Press, Oxford, UK.

Christian, H. J., et al. (2003), Global frequency and distribution of lightning as observed from space by the Optical Transient Detector, *J. Geophys. Res.*, *108*(D1), 4005, doi:10.1029/2002JD002347.

de la Beaujardière, O., et al. (2004), C/NOFS: A mission to forecast scintillations, *J. Atmos. Sol. Terr. Phys.*, *66*, 1573–1591.

Füllekrug, M., and A. C. Fraser-Smith (1997), Global lightning and climate variability inferred from ELF magnetic field variations, *Geophys. Res. Lett.*, *24*, 2411–2414, doi:10.1029/97GL02358.

Fuller-Rowell, T. J. (1998), The "thermospheric spoon": A mechanism for the semiannual density variation, *J. Geophys. Res.*, *103*(A3), 3951–3956.

Garcia, R. R., T. I. Dunkerton, R. S. Lieberman, and R. A. Vincent (1997), Climatology of the semiannual oscillation of the tropical middle atmosphere, *J. Geophys. Res.*, *102*, 26,019–26,032.

Grimalsky, V., S. Koshevaya, A. Kotsarenko, and R. P. Enriquez (2005), Penetration of the electric and magnetic field components of Schumann resonances into the ionosphere, *Ann. Geophys.*, *23*, 2559–2564, doi:10.5194/angeo-23-2559-2005.

Hirota, I. (1980), Observational evidence of the semiannual oscillation in the tropical middle atmosphere – A review, *Pure Appl. Geophys.*, *118*, 217–238, doi:10.1007/BF01586452.

Kandalgaonkar, S. S., M. I. R. Tinmaker, J. R. Kulkarni, A. Nath, M. K. Kulkarni, H. K. Trimbake (2005), Spatio-temporal variability of lightning activity over the Indian region, *J. Geophys. Res.*, *110*, D11108, doi:10.1029/2004JD005631.

Klenzing, J., F. Simões, S. Ivanov, R. A. Heelis, D. Bilitza, R. Pfaff, and D. Rowland (2011), Topside equatorial ionospheric density and composition during and after extreme solar minimum, *J. Geophys. Res.*, *116*, A12330, doi:10.1029/2011JA017213.

Madden, T., and W. Thompson (1965), Low-frequency electromagnetic oscillations of Earth-ionosphere cavity, *Rev. Geophys.*, *3*, 211–254, doi:10.1029/RG003i002p00211.

Märcz, F., G. Sátori, and B. Zieger (1997), Variations in Schumann resonances and their relation to atmospheric electric parameters at Nagycenk station, *Ann. Geophys.*, *15*, 1604–1614.

Mayr, H. G., J. G. Mengel, K. L. Chan, and H. S. Porter (1998), Seasonal variations of the diurnal tide induced by gravity wave filtering, *Geophys. Res. Lett.*, *25*, 943–946.

Meek, C. E., I. M. Reid, and A. H. Manson (1985), Observations of mesospheric wind velocities. 2. Cross sections of power spectral density for 48–8 hours, 8–1 hours, and 1 hour to 10 min over 60–110 km for 1981, *Radio Sci.*, *20*, 1383–1402.

Mikhailov, A. V., and L. Perrone (2011), On the mechanism of seasonal and solar cycle NmF2 variations: A quantitative estimate of the main parameters contribution using incoherent scatter radar observations, *J. Geophys. Res.*, *116*, A03319, doi:10.1029/2010JA016122.

Nickolaenko, A. P., and M. Hayakawa (2002), *Resonances in the Earth-Ionosphere Cavity*, Kluwer Acad, Dordrecht, Netherlands.

Nickolaenko, A. P., and L. M. Rabinowicz (1995), Study of the annual changes of global lightning distribution and frequency variations of the first Schumann resonance mode, *J. JATP.*, *57*, 1345–1348, doi:10.1016/0021-9169(94)00114-4.

Paetzold, H. K., and H. Zschorner (1961), An annual and a semiannual variation of the upper air density, *Pure Appl. Geophys.*, *48*, 85–92.

Pfaff, R., et al. (2010), Observations of DC electric fields in the low-latitude ionosphere and their variations with local time, longitude, and plasma density during extreme solar minimum, *J. Geophys. Res.*, *115*, A12324, doi:10.1029/2010JA016023.

Picone, J. M., A. E. Hedin, D. P. Drob, and A. C. Aikin (2002), NRLMSISE-00 empirical model of the atmosphere: Statistical comparisons and scientific issues, *J. Geophys. Res.*, *107*(A12), 1468, doi:10.1029/2002JA009430.

Reed, R. J. (1966), Zonal wind behavior in equatorial stratosphere and lower mesosphere, *J. Geophys. Res.*, *71*, 4223–4233.

Richards, P. G. (2001), Seasonal and solar cycle variations of the ionospheric peak electron density: Comparison of measurement and models, *J. Geophys. Res.*, *106*, 12,803–12,819, doi:10.1029/2000JA000365.

Rishbeth, H., and C. S. G. K. Setty (1961), The F-layer at sunrise, *J. Atmos. Sol. Terr. Phys.*, *20*, 263–276, doi:10.1016/0021-9169(61)90205-7.

Rishbeth, H., I. C. F. Müller-Wodarg, L. Zou, T. J. Fuller-Rowell, G. H. Millward, R. J. Moffett, D. W. Idenden, and A. D. Aylward (2000), Annual and semiannual variations in the ionospheric F2-layer: II. Physical discussion, *Ann. Geophys.*, *18*, 945–956, doi:10.1007/s00585-000-0945-6.

Russell, C. T., and R. L. McPherron (1973), Semiannual variation of geomagnetic activity, *J. Geophys. Res.*, *78*, 92–108, doi:10.1029/JA078i001p00092.

Sátori, G., and B. Zieger (1996), Spectral characteristics of Schumann resonances observed in Central Europe, *J. Geophys. Res.*, *101*(D23), 29,663–29,669, doi:10.1029/96JD00549.

Sekiguchi, M., M. Hayakawa, A. P. Nickolaenko, and Y. Hobara (2006), Evidence on a link between the intensity of Schumann resonance and global surface temperature, *Ann. Geophys.*, *24*, 1809–1817.

Sentman, D. D., and B. J. Fraser (1991), Simultaneous observations of Schumann resonances in California and Australia – Evidence for intensity modulation by the local height of the D region, *J. Geophys. Res.*, *96*, 15,973–15,983, doi:10.1029/91JA01085.

Sethi, N. K., M. K. Goel, and K. K. Mahajan (2002), Solar cycle variations of foF2 from IGY to 1990, *Ann. Geophys.*, *20*, 1677–1685.

Simões, F., R. F. Pfaff, and H. Freudenreich (2011), Observation of Schumann resonances in the Earth's ionosphere, *Geophys. Res. Lett.*, *38*, L22101, doi:10.1029/2011GL049668.

Simões, F., R. F. Pfaff, J.-J. Berthelier, and J. Klenzing (2012a), A review of low frequency electromagnetic wave phenomena related to tropospheric-ionospheric coupling mechanisms, *Space Sci. Rev.*, *168*, 551–593, doi:10.1007/s11214-011-9854-0.

Simões, F., et al. (2012b), Detection of ionospheric Alfvén resonator signatures in the equatorial ionosphere, *J. Geophys. Res.*, *117*, A11305, doi:10.1029/2012JA017709.

Thampi, S. V., M. Yamamoto, R. T. Tsunoda, Y. Otsuka, T. Tsugawa, J. Uemoto, and M. Ishii (2009), First observations of large-scale wave structure and equatorial spread F using CERTO radio beacon on the C/NOFS satellite, *Geophys. Res. Lett.*, *36*, L18111, doi:10.1029/2009GL039887.

Williams, E. R. (1994), Global circuit response to seasonal variations in global surface air temperature, *Mon. Weather Rev.*, *122*, 1917–1929.